

## Field-Dependent Thermal Transport in the Haldane Chain Compound NENP

A. V. Sologubenko,<sup>1</sup> T. Lorenz,<sup>1</sup> J. A. Mydosh,<sup>1</sup> A. Rosch,<sup>2</sup> K. C. Shortsleeves,<sup>3</sup> and M. M. Turnbull<sup>3</sup>

<sup>1</sup>*II. Physikalisches Institut, Universität zu Köln, 50937 Köln, Germany*

<sup>2</sup>*Institut für Theoretische Physik, Universität zu Köln, 50937 Köln, Germany*

<sup>3</sup>*Carlson School of Chemistry and Biochemistry, Clark University, Worcester, Massachusetts 01610, USA*

(Received 24 December 2007; revised manuscript received 6 February 2008; published 2 April 2008)

We present a study of the magnetic field-dependent thermal transport in the spin  $S = 1$  chain material  $\text{Ni}(\text{C}_2\text{H}_8\text{N}_2)_2\text{NO}_2(\text{ClO}_4)$  (NENP). The measured thermal conductivity is found to be very sensitive to the field-induced changes in the spin excitation spectrum. The magnetic contribution to the total heat conductivity is analyzed in terms of a quasiparticle model, and we obtain a temperature and momentum independent mean free path. This implies that the motion of quasiparticles is effectively three dimensional despite the tiny interchain coupling.

DOI: [10.1103/PhysRevLett.100.137202](https://doi.org/10.1103/PhysRevLett.100.137202)

PACS numbers: 75.40.Gb, 66.70.-f, 75.47.-m

The recent theoretical interest concerning heat transport in one dimensional (1D) spin systems (see review article [1] and the most recent papers [2–8]) was greatly stimulated by observations of a large spin thermal conductivity  $\kappa_s$  in two-leg Heisenberg  $S = 1/2$  ladder compounds  $(\text{La, Sr, Ca})_{14}\text{Cu}_{24}\text{O}_{41}$  at high temperatures, with the mean free path of spin excitations  $l$  reaching  $3000 \text{ \AA}$  [9–11]. However, experiments on several Heisenberg  $S = 1$  chain compounds [12–14] provided evidence for considerably lower  $\kappa_s$ , with  $l \leq 60 \text{ \AA}$ . This is surprising because the  $S = 1$  chain model and the  $S = 1/2$  ladder model are essentially equivalent [15]. Both adopt a spin liquid state with exponentially decaying correlations and an energy gap in the spin excitation spectrum.

The spin thermal conductivity  $\kappa_s$  at a finite frequency  $\omega$  can be decomposed into a singular and a regular part

$$\text{Re } \kappa_s(\omega) = D_{\text{th}}\delta(\omega) + \kappa_{\text{reg}}(\omega), \quad (1)$$

where  $D_{\text{th}}$  is the thermal Drude weight. In our experiment, we measure the dc conductivity  $\text{Re}\kappa_s(\omega = 0)$ . For integrable models and continuum field theories, heat transport is ballistic even at finite temperature  $T$ ,  $D_{\text{th}} > 0$ , as conservation laws prohibit the decay of the heat current. Both extrinsic sources of scattering, such as defects and phonons, and intrinsic spin-spin interactions which are not integrable, render the heat conductivity finite [1–7, 16, 17].

Measurements of the thermal conductivity in external magnetic fields, which can strongly modify the spin excitation spectrum, offer detailed information on scattering mechanisms limiting  $\kappa_s$ . However, magnetic fields typically available are too weak to noticeably influence the spectrum of spin excitations in the previously investigated [12–14]  $S = 1$  chain materials  $\text{AgVP}_2\text{S}_6$  and  $\text{Y}_2\text{BaNiO}_5$  with strong intrachain exchange  $J > 250 \text{ K}$ .

In this Letter, we present results on field-dependent heat transport in one of the model low- $J$   $S = 1$  chain materials,  $\text{Ni}(\text{C}_2\text{H}_8\text{N}_2)_2\text{NO}_2(\text{ClO}_4)$ , *viz.* NENP. The mean free path of the spin excitations, evaluated from our data, is large and

temperature-independent allowing us to identify the most relevant scattering mechanism. The heat transport at low temperatures is determined by rare defects, cutting the spin chains into segments, and not by the intrinsic interactions.

NENP crystallizes in the orthorhombic  $Pnma$  space group with lattice parameters  $a = 15.223 \text{ \AA}$ ,  $b = 10.300 \text{ \AA}$ , and  $c = 8.295 \text{ \AA}$  [18]. The  $S = 1$  spins of  $\text{Ni}^{2+}$  form chains along the  $b$  axis with exchange constant  $J \approx 43 \text{ K}$  [19], while the interaction  $J'$  between the chains is much weaker ( $J'/J \sim 8 \times 10^{-4}$  according to [20]). Therefore, low-temperature 3D ordering is neither expected nor observed. Neglecting the interchain interaction for the moment, the appropriate Hamiltonian is

$$H = \sum_i \{ JS^i S^{i+1} + D(S_z^i)^2 + E[(S_x^i)^2 - (S_y^i)^2] + \mu_B \mathbf{S}^i \cdot \mathbf{g}\mathbf{B} \}, \quad (2)$$

where  $D$  and  $E$  are single-ion anisotropy constants,  $B$  is the magnetic field, and  $\mathbf{g}$  is the gyromagnetic tensor. In an ideal isotropic antiferromagnetic (AFM)  $S = 1$  chain, the excitations are triply degenerate with a gap  $\Delta = 0.41 \text{ J}$  at the AFM wave vector  $k_{\text{AF}} = \pi/d$ , where  $d = b/2$  is the distance between neighboring spins along the chain. In NENP, the strong planar anisotropy and weak orthorhombic anisotropy ( $D/J = 0.2$  and  $E/J \approx 0.01$  [18, 21]) split  $\Delta$  into three gaps  $\Delta_i$  ( $i = 1, 2, 3$ ) with the zero-field values  $\Delta_1^0 \approx 29 \text{ K}$ ,  $\Delta_2^0 = 14.3 \text{ K}$ , and  $\Delta_3^0 = 12.2 \text{ K}$  [20]. With increasing  $B \parallel b$ ,  $\Delta_1$  stays constant,  $\Delta_2$  increases, and  $\Delta_3$  decreases such that it should close at the critical field  $B_c \approx 10 \text{ T}$  and the system should enter a gapless Luttinger liquid (LL) state for  $B > B_c$  [22]. This does not happen, however, because the chemical environment of every second Ni atom along the chain is oriented in a different direction [23]. This alternating tilting introduces an additional term  $\sum_i (-1)^i \mu_B \mathbf{S}^i \cdot \mathbf{g}_{\text{st}} \mathbf{B}$  in the Hamiltonian Eq. (2), where the staggered transverse field  $B_{\text{st}} = |\mathbf{g}_{\text{st}} \mathbf{B}|$  is proportional to the homogeneous field  $B$ . As a consequence, the gap remains finite at  $B = B_c$  and increases above  $B_c$ .

The crystals of NENP used for our experiments were grown as described in Ref. [24]. One crystal of dimensions  $1.1 \times 3 \times 0.5 \text{ mm}^3$  with the longest dimension along the  $b$  axis was used for the measurements of the thermal conductivity along the spin chains. A sample of dimensions  $1.8 \times 0.8 \times 1.4 \text{ mm}^3$  for measurements perpendicular to the chains was cut from another crystal. For the thermal conductivity measurements, we employed a standard steady state method with the same arrangement of the thermometers and heater as described in Ref. [25]. The experiments were performed in the temperature range between 0.3 and 50 K in magnetic fields up to 16 T applied parallel to the chain direction.

The thermal conductivity  $\kappa(T)$  both parallel ( $\kappa^{\parallel}$ ) and perpendicular ( $\kappa^{\perp}$ ) to the chain direction in zero field and in  $B = 8.2 \text{ T}$  are shown in Fig. 1(a). The relative changes of  $\kappa^{\parallel}$  as a function of magnetic field  $\kappa^{\parallel}(B)/\kappa^{\parallel}(0)$  at several constant temperatures are displayed in Fig. 1(b). The striking observation is that a magnetic field leads to a strong enhancement of the thermal conductivity up to 5 times its zero-field value. This strong enhancement is restricted to the direction parallel to the chains. The small increase of  $\kappa^{\perp}(B)$  can easily be attributed to a less than  $1^\circ$  deviation of the heat flow direction from being exactly perpendicular to the  $b$  axis.

The total thermal conductivity of a magnetic insulator can be represented as  $\kappa = \kappa_{\text{ph}} + \kappa_s$ , where the two terms on the right-hand side correspond, respectively, to the phononic and magnetic contributions to the heat transport (possible spin-phonon drag contributions are included in  $\kappa_s$ ). The spin excitation spectrum at  $B = 0$  is gapped with the smallest gap  $\Delta_3 = 12.2 \text{ K}$ ; therefore, at  $T \ll \Delta_3$ , both spin thermal conductivity and phonon-spin scattering are negligible. With increasing  $B$  at a constant temperature,  $\Delta_3(B)$  decreases, and the number of thermally activated spin excitations increases. Therefore,  $\kappa_s(B)$  should increase, while  $\kappa_{\text{ph}}(B)$  should decrease because of the growing phonon scattering by spin excitations. Because of the quasi-1D nature of the spin system in NENP,  $\kappa_s^{\perp}$  is small and  $\kappa^{\perp} \approx \kappa_{\text{ph}}^{\perp}$ . Thus, the observed negligible influence of

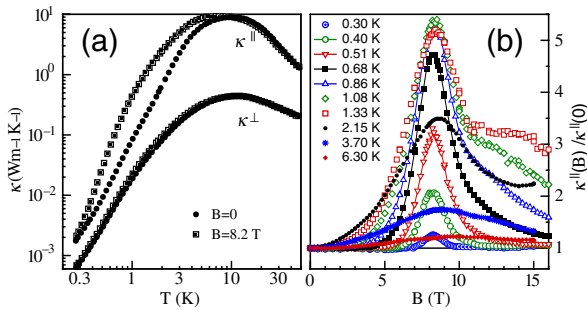


FIG. 1 (color online). (a) Thermal conductivity of NENP parallel and perpendicular to the spin chains as a function of temperature at  $B = 0$  and  $B = 8.2 \text{ T}$ . (b) The relative change of the thermal conductivity of NENP parallel to the spin chains as a function of magnetic field at several constant temperatures.

the magnetic field on  $\kappa^{\perp}$  suggests that spin-phonon scattering is weak. The increase of  $\kappa^{\parallel}(B)$  in fields  $0 < B < B_c$  clearly demonstrates that all field-induced changes in  $\kappa^{\parallel}$  originate from  $\kappa_s$ .

A salient feature of the curves shown in Fig. 1(b) is that for all temperatures below about 1.5 K there is a region of low fields where  $\kappa^{\parallel}(B)/\kappa^{\parallel}(0)$  are practically field-independent. This means that below about 1.5 K  $\kappa^{\parallel}(B = 0)$  is purely phononic. Therefore, by subtracting the zero-field values from  $\kappa^{\parallel}$  at these temperatures we obtain a good estimate of  $\kappa_s(B)$ .

We have measured  $\kappa^{\parallel}(T)$  below 1.5 K at several constant fields. The spin contribution  $\kappa_s(B, T) \equiv \kappa^{\parallel}(B, T) - \kappa^{\parallel}(0, T)$  is shown in Fig. 2. For a quantitative analysis of the data, we consider the heat transport associated with excitations from the singlet ground state to the lowest triplet branch. As the energy gaps for the other two branches of the triplet either increase with  $B$  or stay constant, their contribution to the heat transport below  $T \approx 1.5 \text{ K}$  can be disregarded. The interaction between chains is very weak in comparison with the intrachain interaction; nevertheless, it still leads to a dispersion perpendicular to the  $b$  axis with a bandwidth of about 2 K and 0.8 K along the  $a$  and  $c$  axes, respectively [20,26]. The dispersion we use in order to analyze  $\kappa_s$  in low fields (hence the subscript “ $lf$ ”)  $1 \text{ T} \leq B \leq 6 \text{ T}$  is given by

$$\begin{aligned} \varepsilon_{lf}(\mathbf{k}) = & \{[(\Delta_2^0 + \Delta_3^0)/2]^2 + V^2(k_b d - \pi)^2 \\ & + (\Delta E_a)^2[(1 + \cos k_a a)/2]^2 \\ & + (\Delta E_c)^2[(1 + \cos k_c c)/2]^2\}^{1/2} - g_b \mu_B B, \end{aligned} \quad (3)$$

with constants  $\Delta_2^0 = 14.3 \text{ K}$ ,  $\Delta_3^0 = 12.2 \text{ K}$ ,  $\Delta E_a = 7.5 \text{ K}$ , and  $\Delta E_c = 5.0 \text{ K}$  taken from neutron scattering experiments [20,26] and  $g_b = 2.15$  from an ESR study [19]. The value of  $V = 2.49 \text{ J}$ , used in the analysis, is predicted by theory [27] and is confirmed by the inelastic neutron scattering measurements [20,28]. Equation (3) describes

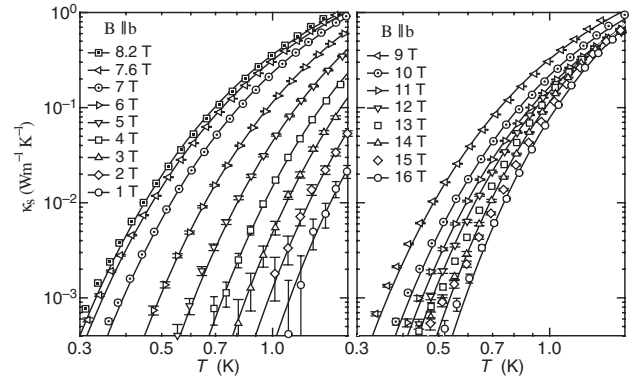


FIG. 2. Magnetic contribution to the thermal conductivity of NENP parallel to the spin chains as a function of temperature at several constant fields. The solid lines represent the calculated  $\kappa_s$  (see text). The error bars arise from the uncertainty in subtraction of  $\kappa_{\text{ph}}$  from the total measured thermal conductivity.

correctly the linear-in- $B$  decrease of the energy gap at  $\mathbf{q} = (0, \pi/d, 0)$  between 1 and 6 T observed in the ESR experiment [19], but does not account for deviations at higher fields caused by the influence of the aforementioned transverse staggered field.

Within the Boltzmann equation approximation, the spin thermal conductivity parallel to the chain direction is represented by

$$\kappa_s = \frac{n}{\hbar \pi^3} l \int_0^{\pi/a} dk_a \int_0^{\pi/c} dk_c \int_0^{\pi/b} dk_b \frac{df}{dT} \varepsilon(\mathbf{k}) \frac{d\varepsilon(\mathbf{k})}{dk_b} dk_b, \quad (4)$$

where  $n = 4$  is the number of spins in the unit cell of NENP,  $f$  is the distribution function,  $\varepsilon(\mathbf{k})$  is the energy, and  $l$  is the mean free path of spin excitations. In Eq. (4), we use the Fermi distribution  $f = [\exp(\varepsilon/k_B T) + 1]^{-1}$  (taking into account the hard-core repulsion of the 1D excitations) [29], but as the temperature is well below the gap, one can equally well use a Boltzmann or Bose distribution.

In the field region  $1 \text{ T} \leq B \leq 6 \text{ T}$ , where  $\varepsilon(\mathbf{k}) = \varepsilon_{lf}(\mathbf{k})$ , the only unknown parameter in Eq. (4) is  $l$ . Thus, the mean free path,  $l(B, T)$ , as a function of  $B$  and  $T$  can be extracted from the experimental data of Fig. 2 and is shown in Fig. 3. Within the experimental accuracy, the mean free path is independent of both  $T$  and  $B$ , with the average value  $\bar{l} = 0.75 \pm 0.1 \mu\text{m}$ . Remarkably,  $\bar{l}$  for NENP is as large as the highest values of the mean free path found for  $S = 1/2$  Heisenberg chains and ladders [10,25,30], where impurities are the main source of scattering for spin excitations at low  $T$ . Both for spin-spin and spin-phonon scattering, the mean free path is expected to increase rapidly with decreasing  $T$  [3]. We therefore conclude that, at least at  $T < 0.04 \text{ J}$ , scattering by defects and not the intrinsic interactions determine  $\kappa_s$ . A mean free path due to the intrinsic

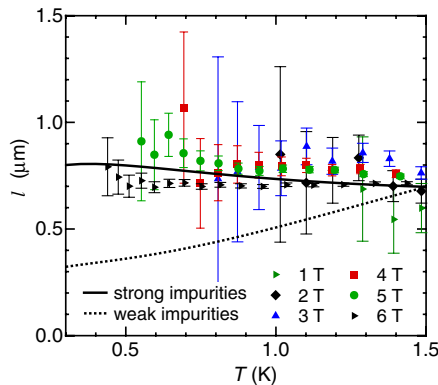


FIG. 3 (color online). Mean free path of spin excitations, calculated for  $1 \text{ T} \leq B \leq 6 \text{ T}$ . The error bars correspond to those of  $\kappa_s$  shown in Fig. 2. An approximately constant mean free path can be obtained from a model (solid line) where strong impurities effectively cut the spin chains into segments of length  $l$ . In contrast, the data cannot be described (dashed line) by weak fluctuations of  $J$ .

processes is theoretically expected to be huge [2] as Umklapp processes which relax momentum are exponentially suppressed for  $T \ll J$ .

A field and temperature independent mean free path cannot be obtained from a purely 1D model. For both weak and strong impurities, one expects [25] in one dimension a momentum dependent mean free path proportional to the square of the velocity,  $l_k \propto v_k^2$ , implying effectively a variation of  $l$  linear with  $T$ . The situation is, however, completely different when one takes the tiny three dimensional coupling between the chains into account. If spin excitations can pass “strong” impurities, which effectively cut the chains into segments, by hopping to the next chain instead of tunneling through the defect, one naturally obtains a mean free path given by the distance of the defects. We have calculated the weak  $T$  dependence of  $l$  (solid line in Fig. 3) assuming a small density of local, infinitely strong potential scatterers in a model defined by the dispersion relation (3) for a gap  $\Delta$  of 5 K (for  $T \ll \Delta$  the result is almost independent of  $\Delta$ ). Such a simple calculation to linear order in the density of defects is valid as the interchain coupling  $J'$  (or more precisely the bandwidth in perpendicular direction) is much larger than the inverse of the time needed by a spin excitation with energy  $T$  to propagate to the next defect,  $J' > \sqrt{TJ}d/l$ .

The calculations for the mean free path dominated by strong impurities describe the data very well (solid line in Fig. 3). This is not the case when one assumes that small fluctuations  $\delta J \approx T$  of  $J$  dominate transport (dashed line in Fig. 3). In the latter case, the scattering rate is proportional to the density of state [obtained again from Eq. (3)].

The model we used for the low-field calculations fails to describe  $\kappa_s(B, T)$  at  $B > 6 \text{ T}$ . This is illustrated in

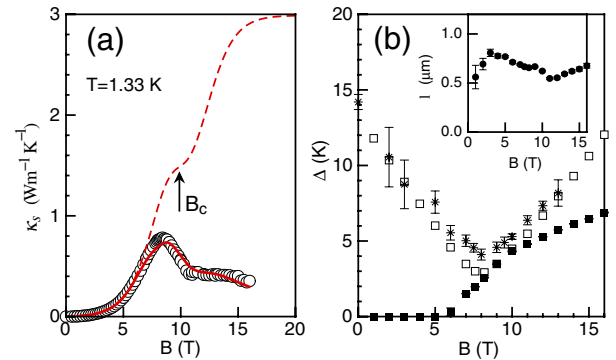


FIG. 4 (color online). (a)  $\kappa_s(B)$  calculated for  $T = 1.33 \text{ K}$  with (solid line) and without (dashed line) consideration of the staggered transverse field. The open circles represent the experimental data. (b) The open squares are the minimum energy gap  $\Delta_{\min}$  estimated in our analysis. For comparison, the energy gap obtained from specific heat measurements from Ref. [32] are shown (stars). The solid squares are the fitted values for  $\Delta_{\perp}$  (the vanishing of  $\Delta_{\perp}$  below 6 T may be an artifact of the fitting procedure as  $\Delta_{\min}$  depends very little on  $\Delta_{\perp}$  in this regime). Inset: The fit values of the mean free path of spin excitations.

Fig. 4(a), where the dashed line is  $\kappa_s(B)$  calculated for a constant temperature  $T \ll J$  using Eqs. (3) and (4) with  $l = \bar{l}$ . The calculated  $\kappa_s(B)$  shows an increase when  $B$  approaches the LL state from the gapped state, with a plateaulike feature at  $B_c$  broadened by the interchain interaction. This is the expected generic behavior for a 1D spin system near a quantum phase transition from a gapped to a gapless state and has, indeed, been observed for the  $S = 1/2$  chain compound CuPzN in [25]. The different behavior of NENP for high fields arises obviously from the energy gap induced by the staggered field.

We have fitted Eq. (4) to the  $\kappa_s(T)$  data presented in Fig. 2 using a modified dispersion relation  $\varepsilon(\mathbf{k}) = \sqrt{\Delta_{\perp}^2 + \varepsilon_{lf}^2(\mathbf{k})}$ , where  $\varepsilon_{lf}(\mathbf{k})$  is given by Eq. (3) and the energy gap  $\Delta_{\perp}$  is induced by the staggered field. A similar heuristic fitting formula has, e.g., been used in Ref. [31] to describe the  $S = 1/2$  chain compound  $\text{CuCl}_2 \cdot 2[(\text{CD}_3)_2\text{SO}]$  where, similar to NENP, a staggered field induced by a uniform magnetic field leads to a finite gap in the spin excitation spectrum. For each value of  $B$  between 1 and 16 T, Eq. (4) was fitted to the experimental  $\kappa_s(T)$  data, shown in Fig. 2, with two free parameters  $l$  and  $\Delta_{\perp}$ , assuming that  $l$  is  $T$ -independent for each  $B$ . The resulting  $\kappa_s(T)$  curves are shown in Fig. 2. The fit values for  $\Delta_{\perp}(B)$  are shown by solid squares in Fig. 4(b), the data for  $l(B)$  are presented in the inset of Fig. 4(b). The solid line in Fig. 4(a) is calculated using these data for  $l(B)$  and  $\Delta_{\perp}(B)$ . As shown in Fig. 4(b), there is an agreement between our data for the minimum energy gap  $\Delta_{\min} \equiv \{[(\Delta_2^0 + \Delta_3^0)/2 - g_b \mu_B B]^2 + \Delta_{\perp}^2\}^{1/2}$  at  $\mathbf{k} = (\pi/a, \pi/d, \pi/c)$  and the data for the energy gap obtained from the specific heat measurements [32]. The essential result is that the mean free path  $l$  remains close to its low-field value  $\bar{l} = 0.75 \mu\text{m}$  in the entire 1–16 T field region. This is again consistent with the notion of a mean free path determined by strong impurities.

In summary, from our measurements of the anisotropic thermal conductivity of the  $S = 1$  Haldane chain compound NENP, we identify a large magnetic contribution along the spin chain direction. The mean free path of spin excitations is orders of magnitude larger than previously observed for other  $S = 1$  chain materials and of the same order of magnitude as in the best  $S = 1/2$  chain and ladder compounds. We have argued that the absence of a temperature and field dependence of the mean free path can be explained by rare defects, which effectively cut the spin chains into segments, in combination with a tiny interchain coupling. The measured values of spin thermal conductivity may also serve as a lower limit for future theoretical estimates of the intrinsic diffusive contribution to the heat transport in  $S = 1$  AFM chains at low temperatures.

We acknowledge useful discussions with A. Altland, D. I. Khomskii, M. Garst, E. Shimshoni, M. Vojta, and S.

Zvyagin. This work was supported by the DFG through No. SFB 608.

- 
- [1] X. Zotos and P. Prelovsek, in *Strong Interactions in Low Dimensions*, edited by D. Baeriswyl and L. Degiorgi (Kluwer Academic Publishers, Dordrecht, 2004), p. 347.
  - [2] P. Jung and A. Rosch, Phys. Rev. B **75**, 245104 (2007); P. Jung, R. W. Helmes, and A. Rosch, Phys. Rev. Lett. **96**, 067202 (2006).
  - [3] E. Boulat *et al.*, Phys. Rev. B **76**, 214411 (2007); E. Shimshoni, N. Andrei, and A. Rosch, Phys. Rev. B **68**, 104401 (2003).
  - [4] A. V. Savin, G. P. Tsironis, and X. Zotos, Phys. Rev. B **75**, 214305 (2007).
  - [5] K. Louis, P. Prelovšek, and X. Zotos, Phys. Rev. B **74**, 235118 (2006).
  - [6] F. Heidrich-Meisner, A. Honecker, and W. Brenig, Phys. Rev. B **71**, 184415 (2005).
  - [7] A. V. Rozhkov and A. L. Chernyshev, Phys. Rev. Lett. **94**, 087201 (2005).
  - [8] T. Sakai and S. Yamamoto, J. Phys. Soc. Jpn. Suppl. **74**, 191 (2005).
  - [9] A. V. Sologubenko *et al.*, Phys. Rev. Lett. **84**, 2714 (2000).
  - [10] C. Hess *et al.*, Phys. Rev. B **64**, 184305 (2001).
  - [11] K. Kudo *et al.*, J. Phys. Chem. Solids **62**, 361 (2001).
  - [12] A. V. Sologubenko *et al.*, Phys. Rev. B **68**, 094432 (2003).
  - [13] K. Kordonis *et al.*, Phys. Rev. Lett. **97**, 115901 (2006).
  - [14] T. Kawamata *et al.*, J. Magn. Magn. Mater. **310**, 1212 (2007).
  - [15] S. R. White, Phys. Rev. B **53**, 52 (1996).
  - [16] E. Orignac, R. Chitra, and R. Citro, Phys. Rev. B **67**, 134426 (2003).
  - [17] J. Karadamoglou and X. Zotos, Phys. Rev. Lett. **93**, 177203 (2004).
  - [18] A. Meyer *et al.*, Inorg. Chem. **21**, 1729 (1982).
  - [19] M. Sieling *et al.*, Phys. Rev. B **61**, 88 (2000).
  - [20] L. P. Regnault, I. Zaliznyak, J. P. Renard, and C. Vettier, Phys. Rev. B **50**, 9174 (1994).
  - [21] T. Delica, K. Kopinga, H. Leschke, and K. K. Mon, Europhys. Lett. **15**, 55 (1991).
  - [22] R. M. Konik and P. Fendley, Phys. Rev. B **66**, 144416 (2002).
  - [23] M. Chiba *et al.*, Phys. Rev. B **44**, 2838 (1991).
  - [24] V. C. Long *et al.*, Phys. Rev. B **76**, 024439 (2007).
  - [25] A. V. Sologubenko *et al.*, Phys. Rev. Lett. **98**, 107201 (2007).
  - [26] I. A. Zaliznyak, D. C. Dender, C. Broholm, and D. H. Reich, Phys. Rev. B **57**, 5200 (1998).
  - [27] E. S. Sorensen and I. Affleck, Phys. Rev. Lett. **71**, 1633 (1993).
  - [28] S. L. Ma *et al.*, Phys. Rev. Lett. **69**, 3571 (1992).
  - [29] H. Huang and I. Affleck, Phys. Rev. B **69**, 184414 (2004).
  - [30] A. V. Sologubenko, H. R. Ott, G. Dhalenne, and A. Revcolevschi, Europhys. Lett. **62**, 540 (2003).
  - [31] M. Kenzelmann *et al.*, Phys. Rev. B **71**, 094411 (2005).
  - [32] T. Kobayashi *et al.*, J. Phys. Soc. Jpn. **61**, 1772 (1992).